Hydrophobic−Electrostatic Balance Driving the LCST Offset Aggregation−Redissolution Behavior of *N*-Alkylacrylamide-Based Ionic Terpolymers

Paula M. López-Pérez,[†,‡,§] Ricardo M. P. da Silva,[*,†,‡] Iva Pashkuleva,[†,‡] Francisco Parra,[§,⊥] Rui L. Reis,[†,‡] and Julio San Roman[§,⊥]

[†]*3B's Research Group − Biomaterials, Biodegradables and Biomimetics, University of Minho Headquarters of the European Institute of Excellence on Tissue Engineering and Regenerative Medicine, AvePark, 4806-909 Taipas, Guimarães, Portugal,* [‡]*IBB − Institute for Biotechnology and Bioengineering, PT Government Associated Laboratory, Braga, Portugal,* [§]*Institute of Polymer Science and Technology, CSIC. C/Juan de la Cierva, 3, 28006-Madrid, Spain, and* [⊥]*CIBER-BBN, Spain*

A series of random terpolymers composed of *N*-isopropylacrylamide (NIPAAm), 2-acrylamido-2-methyl-1-propanesulfonic acid (AMPS), and *N-tert*-butylacrylamide (NTBAAm) monomers were synthesized by free radical polymerization. The molar fraction of the negatively charged monomer (AMPS) was maintained constant (0.05) for all studied terpolymer compositions. Turbidity measurements were used to evaluate the influence of the relative amount of NIPAAm and NTBAAm, polymer concentration, and solution ionic strength on the cloud point and redissolution temperatures (macroscopic phase separation). Dynamic light scattering (DLS) was employed to elucidate some aspects regarding the molecular scale mechanism of the temperature-induced phase separation and to determine the low critical solution temperature (LCST). The aqueous solutions of terpolymers remained clear at all studied temperatures; turbidity was only observed in the presence of NaCl. The cloud point temperature (CPT) determined by turbidimetry was found to be systematically much higher than the LCST determined by DLS; nanosized aggregates were observed at temperatures between the LCST and the CPT. Both CPT and LCST decreased when increasing the molar ratio of NTBAAm (increased hydrophobicity). It was found that above a critical molar fraction of NTBAAm (0.25−0.30) the aggregation rate suddenly decreased. Polymers with NTBAAm content lower than 0.25 showed a fast macroscopic phase separation, but the formed large aggregates are disaggregating during the cooling ramp at temperatures still higher than the LCST. On the contrary, polymers with NTBAAm contents above 0.30 showed a slow macroscopic phase separation, and the formed large aggregates only redissolved when LCST was reached. These differences were explained on the basis of a delicate balance between the electrostatic repulsion and the hydrophobic attractive forces, which contribute cooperatively to the formation of metastable nanosized aggregates.

Introduction

Several polymers that are soluble in a certain solvent at low temperature undergo phase separation above a critical temperature value known as lower critical solution temperature (LCST). At the macroscopic level the phenomenon is similar for all polymer solutions that present LCST; a clear solution becomes "milky" upon heating (cloud point). Polymers showing this behavior in aqueous solution, such as poly(*N*-isopropylacrylamide) (pNIPAAm) and other *N*-substituted acrylamide polymers, had been extensively studied[1−7] because of their theoretical significance and technological potential. It has been shown that isolated pNIPAAm polymer chains undergo an abrupt conformational transition from expanded and flexible coil to an insoluble compact globule, as the temperature is raised above the Flory Θ-temperature,[2−7] which is the theoretical limit between good and poor solvent regions. The coil-to-globule transition of these synthetic macromolecules provides a simple phenomenological model for many biological systems, such as protein folding, native DNA packing, and network collapse.[8] For example, (i) the molten globule state of proteins has been also observed for single pNIPAAm chains;[3] (ii) when copolymerized with small amounts of acrylic acid, collapsed polymer chains form thermodynamically stable interchain aggregates stabilized by surface charge,[9] resembling protein quaternary structure; (iii) the ability of salts to influence pNIPAAm LCST follows the same trend recurrently found for the precipitation of proteins (salting out), known as the Hofmeister series.[10] From the technological point of view, these polymers have been proposed for applications such as pulsatile drug delivery systems,[11] polymer supports in catalysis and synthesis,[12] biomolecule affinity separation,[13] and nondestructive harvesting in mammalian cell culture,[14,15] just to enumerate a few.

*Corresponding author. E-mail: ricardosilva@dep.uminho.pt.
(1) Liu, H. Y.; Zhu, X. X. *Polymer* **1999**, *40*, 6985.
(2) Graziano, G. *Int. J. Biol. Macromol*. **2000**, *27*, 89.
(3) Wu, C.; Zhou, S. Q. *Phys. Rev. Lett*. **1996**, *77*, 3053.
(4) Wu, C.; Zhou, S. Q. *Macromolecules* **1995**, *28*, 8381.
(5) Wu, C.; Zhou, S. Q. *Macromolecules* **1995**, *28*, 5388.
(6) Kubota, K.; Fujishige, S.; Ando, I. *J. Phys. Chem*. **1990**, *94*, 5154.
(7) Fujishige, S.; Kubota, K.; Ando, I. *J. Phys. Chem*. **1989**, *93*, 3311.

(8) Baysal, B. M.; Karasz, F. E. *Macromol. Theory Simul*. **2003**, *12*, 627.
(9) Qiu, X. P.; Li, M.; Kwan, C. M. S.; Wu, C. *J. Polym. Sci., Part B: Polym. Phys*. **1998**, *36*, 1501.
(10) Zhang, Y. J.; Furyk, S.; Bergbreiter, D. E.; Cremer, P. S. *J. Am. Chem. Soc*. **2005**, *127*, 14505.
(11) Alarcon, C. D. H.; Pennadam, S.; Alexander, C. *Chem. Soc. Rev*. **2005**, *34*, 276.
(12) Bergbreiter, D. E.; Case, B. L.; Liu, Y. S.; Caraway, J. W. *Macromolecules* **1998**, *31*, 6053.
(13) Nagase, K.; Kobayashi, J.; Okano, T. *J. R. Soc. Interface* **2009**, *6*, S293.
(14) da Silva, R. M. P.; Mano, J. F.; Reis, R. L. *Trends Biotechnol*. **2007**, *25*, 577.
(15) Ebara, M.; Yamato, M.; Hirose, M.; Aoyagi, T.; Kikuchi, A.; Sakai, K.; Okano, T. *Biomacromolecules* **2003**, *4*, 344.

In terms of polymer–solvent interactions, the coil-to-globule transition involves combined hydrophobic hydration and hydrogen bonding effects. During phase separation, hydrogen bonds between water molecules and polymer amide groups are disrupted and replaced by intramolecular hydrogen bonds among the dehydrated amide groups.[16,17] If the polymer concentration is not exceptionally low, intrachain condensation is readily followed by aggregation and coalescence of the collapsing globules, prompted by hydrophobic interactions and interchain hydrogen bonding.[4–7,16] The intrachain coil-to-globule transition and the interchain aggregation are two independent, but competing, processes.[4–7,9] Except on extremely diluted solutions, where interactions between different polymer chains are kept at insignificant levels,[3–7] both processes occur concomitantly in most practical situations.

N-Alkyl-substituted polyacrylamides are a class of homopolymers that combine simultaneously in the same monomer hydrophilic amide groups able to form hydrogen bonds with the hydration water and hydrophobic *N*-alkyl groups, forcing hydration water to assume a more organized structure.[18] Thus, it is not surprising that the behavior of a *N*-substituted acrylamide homopolymer in solution depends markedly on the *N*-substituent nature. Whereas the *N*-isopropyl-substituted acrylamide phase separation appears at around 32 °C,[4–7] more hydrophobic substituents lower the LCST and more hydrophilic ones increase the LCST.[1] Moreover, its copolymerization with more hydrophobic or hydrophilic monomers has the same effect on the LCST, providing a suitable route to fine-tune the LCST, by just making polymers with subtle differences in the composition.[1,19–21] Interestingly, a LCST behavior was observed for nonionic copolymers of "very hydrophobic" or "very hydrophilic" *N*-substituted polyacrylamides that produce either completely insoluble or completely soluble homopolymers, respectively.[1] The LCST of these nonionic copolymers could be adjusted between the freezing and boiling points of the aqueous solutions by varying the composition.[1] On the other hand, ionic copolymer gels of *N*-tert-butylacrylamide (NTBAAm) and 2-acrylamido-2-methyl-1-propanesulfonic acid (AMPS) presented a discontinuous phase separation only in a limited compositional range. When the amount of the negatively charged AMPS was increased over a certain limit, the repulsive electrostatic interactions avoided the sudden collapse of the polymer network, and consequently a continuous-type swelling was observed with the temperature increase.[21]

In this study, a series of ionic terpolymers of three different *N*-substituted acrylamide monomers (NIPAAm, NTBAAm, and AMPS) was synthesized, and the effect of NaCl and polymer concentrations in the solution behavior was evaluated. Our interest in ionic thermoresponsive polymers relies on their technological relevance because of their ability to form surfactant-free nanoparticles stabilized by surface charge above the LCST[9] or to interact with oppositely charged macromolecules, allowing for the construction of thermoresponsive polyelectrolyte complexes.[22] AMPS was chosen to afford a negative charge to the terpolymers because it is a strong acid[23] ($pK_a = 1.9$) that dissociates completely in the pH range of most envisaged applications. An

(16) Cheng, H.; Shen, L.; Wu, C. *Macromolecules* **2006**, *39*, 2325.
(17) Schild, H. G.; Tirrell, D. A. *J. Phys. Chem.* **1990**, *94*, 4352.
(18) Tamai, Y.; Tanaka, H.; Nakanishi, K. *Macromolecules* **1996**, *29*, 6761.
(19) Feil, H.; Bae, Y. H.; Jan, F. J.; Kim, S. W. *Macromolecules* **1993**, *26*, 2496.
(20) Mao, H. B.; Li, C. M.; Zhang, Y. J.; Furyk, S.; Cremer, P. S.; Bergbreiter, D. E. *Macromolecules* **2004**, *37*, 1031.
(21) Varghese, S.; Lele, A. K.; Mashelkar, R. A. *J. Chem. Phys.* **2000**, *112*, 3063.
(22) Wong, J. E.; Diez-Pascual, A. M.; Richtering, W. *Macromolecules* **2009**, *42*, 1229.
(23) Travas-Sejdic, J.; Easteal, A. *Polym. Gels Networks* **1997**, *5*, 481.

Chart 1. Poly(NIPAAm-*co*-NTBAAm-*co*-AMPS) Chemical Structure
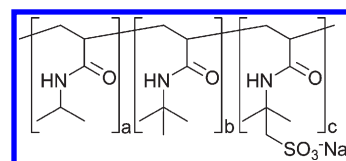
AMPS molar ratio of 0.05 was chosen to ensure a sharp phase separation, since it is reasonably below the limit wherein p(AMPS-*co*-NTBAAm) gels lose their discontinuous phase-separation behavior.[21] Furthermore, the functional sulfonic group position in AMPS gives the terpolymers a continuous structural similarity along the polymer backbone, composed of isopropyl and *tert*-butyl side groups *N*-linked to inner amide groups. The sulfonic groups bound to some of the *tert*-butyl side groups are located on the periphery of the macromolecule (see Chart 1). This avoids the disruption of the continuity of the *N*-alkyl groups, which has been referred in the literature to decrease hydrophobic aggregation force necessary for the cooperative chain collapse, thus decreasing phase-separation sharpness.[15,24] All terpolymers were synthesized containing the same relative amount of AMPS, i.e., containing the same charge. In order to adjust the LCST, terpolymer hydrophobic content was varied by changing NTBAAm to NIPAAm monomer ratio.

Materials and Methods

N-Isopropylacrylamide (NIPAAm, Acros Organics) and 2,2′-azobis(isobutyronitrile) (AIBN) (Fluka) were recrystallized from a *n*-hexane/diethyl ether (5:1) mixture and methanol, respectively. 2-Acrylamido-2-methyl-1-propanesulfonic acid (AMPS) and *N*-tert-butylacrylamide (NTBAAm) were both purchased from Sigma-Aldrich and used as received as all other materials.

Copolymers Synthesis and Characterization. Linear terpolymers p(NIPAAm-*co*-NTBAAm-*co*-AMPS) were synthesized by free-radical copolymerization using AIBN as initiator. The copolymers are designed as $XX/YY/ZZ$, being XX, YY, and ZZ the molar percentages of NIPAAm, NTBAAm, and AMPS in the reaction mixture, respectively. Monomers with a total concentration of 0.5 M were dissolved in an 50:50 isopropanol:water mixture and AIBN (1 mol % with respect to the total monomer) was added to the solution. After degasification of the reactants solution with nitrogen for about 15 min, the reaction vessel was sealed and placed in an oven at 60 °C for 16 h. The solution containing the obtained polymers was neutralized with NaOH, dialyzed against distilled water using dialysis tubes with a cutoff molecular weight of 3500 Da, and freeze-dried.

Terpolymers composition was analyzed by Elemental analyses (Leco CHNS-932) and ^{1}H NMR using CDCl₃ as solvent (Varian Inova 300). Molecular weight and polydispersity were determined by gel permeation chromatography (GPC) using 0.1% (w/v) LiBr solution in DMF as eluent at a flow rate of 0.3 mL min⁻¹ at 70 °C and narrow disperse poly(ethylene glycol) (PEG) as calibration standards.

Turbidity Measurements. The cloud point temperature (CPT) of the polymer solutions was measured in a Varian-Cary 3 UV/vis spectrophotometer, equipped with a Peltier cell holder for temperature control. The turbidity of the solutions was monitored as a function of temperature at 400 nm and under magnetic stirring. Solutions were prepared using distilled water with varying NaCl concentrations. These solutions were expected to be roughly neutral because AMPS is a fairly strong acid and the terpolymers had been previously converted in the salt form.

(24) Aoyagi, T.; Ebara, M.; Sakai, K.; Sakurai, Y.; Okano, T. *J. Biomater. Sci., Polym. Ed.* **2000**, *11*, 101.

Table 1. Copolymers Composition and Molecular Weight

sample	molar fraction in polymer			$M_w/10^3$ (g/mol)	$M_n/10^3$ (g/mol)	M_w/M_n
	NIPAAm[a]	NTBAAm[a]	AMPS[b]			
45/50/5	0.47	0.48	0.04	17.2	6.3	2.7
50/45/5	0.49	0.46	0.04	17.2	6.0	2.6
55/40/5	0.53	0.42	0.06	15.3	5.8	2.6
60/35/5	0.58	0.37	0.04	18.2	6.3	2.9
70/25/5	0.67	0.28	0.04	19.7	6.9	2.8
75/20/5	0.69	0.27	0.05	18.9	7.0	2.7
80/15/5	0.76	0.19	0.05	18.5	7.1	2.6
90/5/5	0.83	0.12	0.05	18.8	7.1	2.7
95/0/5	0.95	0.0	0.05	16.4	6.3	2.6

[a] Calculated by ^1H NMR considering AMPS 5.0%. [b] Calculated by elemental analysis.

Solutions were frozen at −20 °C to ensure complete dissolution. Immediately after melting, solutions were placed in a cuvette, and heating scans were performed between 15 and 80 °C at a scanning rate of 1 °C/min. The first measured point at 15 °C was used as blank which corresponds to the clear polymer solution. The transmittance of the polymer solution at different concentration and ionic strength (adjusted with NaCl) was monitored as a function of temperature. Cooling scans were performed between 80 and 5 °C immediately after heating at the same rate. The aggregation kinetic isotherms were evaluated for an aqueous solution of 60/35/5 (1 g/L) in NaCl (0.154 M). Solutions were frozen before each temperature measurement, and blank was record at 15 °C, as for the temperature scanning experiments. Afterward, the solutions were rapidly heated to set temperature values near and above the CPT, and transmittance was recorded as a function of time.

Dynamic Light Scattering (DLS). Dynamic Light scattering was performed using a Zetasizer NanoZS Instrument (ZEN3600, Malvern Instruments, Worcestershire, UK) equipped with a 4 mW He−Ne laser (λ_0 = 633 nm) and with noninvasive backscattering (NIBS) detection at a scattering angle of 173°. Owing to this configuration, the equipment can decrease the scattered light path length through the sample by adjusting automatically the measuring position, hence reducing multiple scattering for larger particle size, i.e., opaque samples. This is especially useful in colloidal aggregation experiments, where scattered light intensity can rapidly increase several orders of magnitude, because it reduces the need of sample dilution. Both measuring position and attenuator were adjusted automatically before each measurement. The autocorrelation function was converted in a volume-weighted particle size distribution with Dispersion Technology Software 5.06 from Malvern Instruments. The apparent hydrodynamic diameters (D_h) were taken as the mean position of the peak in volume−D_h distributions. The measurements were performed in the temperature range 5−85 °C with a temperature interval of 2 °C and an equilibration time of 2 min. Regarding the stability measurements, samples were initially frozen, melted, and equilibrated at 5 °C inside the measurement cell to ensure complete dissolution. Thereafter, samples were submitted to a temperature jump and measured at constant temperature for 12 h. Terpolymer solutions with varying salt concentration were prepared in ultrapure water and filtered using a 0.20 μm disposable PES membrane filter (TPP, Trasadingen, Switzerland).

Results and Discussion

Several NIPAAm-*co*-NTBAAm-*co*-AMPS copolymers containing different NIPAAm/NTBAAm ratios and a constant 5 mol % of AMPS in the feed were prepared. Their composition and molecular weight are summarized in Table 1. The composition of the copolymers is quite close to the reaction feed composition, according to the expected from the chemical structure of the monomers and reactivity ratios reported in the literature.[25,26] The AMPS molar fraction was experimentally determined to be around 0.05 for all copolymers, and the small differences observed fall under the technique uncertainty. Besides, the small error fluctuations in the AMPS molar fraction do not correlate with the other monomer ratio. Therefore, we can exclude biased effects caused by polymer charge trends when analyzing properties related with the other two monomer frequencies. Moreover, the weight-average molecular weight (M_w) and polydispersity (M_w/M_n), determined by GPC, are also similar for all polymer samples, showing that these parameters are not affected by the monomers feed ratio.

Turbidimetry is a common technique used to estimate the LCST of thermoresponsive polymers in aqueous solutions, motivated by the tendency of polymer molecules to aggregate at the poor solvent region above the Θ-temperature, which causes a marked change in the solution optical properties.[6,7] However, complications might arise from variations in the size of precipitated aggregate and the settling of precipitates, which is especially critical in aged solutions. The cloud point, measured at the onset of the turbidity increases with the temperature, should be an overestimation of the LCST. However, the cloud point can still provide an acceptable estimation of the LCST for a stipulated temperature scanning rate if aggregation kinetics is faster enough. This fact, allied with the experimental simplicity, makes turbidimetry a primary choice in the literature for a fast estimation of the LCST. The concentration of the polymer solution (diluted regimes), the presence of surfactants, or the polymer ionic charge are some of the several factors that might influence aggregation kinetics. Nonetheless, turbidimetry provides a fast way of obtaining valuable information about the macroscopic phase-separation behavior, even if the CPT does not match exactly the coil-to-globule transition. We have characterized our terpolymers solution behavior by means of turbidimetry, and the results were analyzed taking into consideration the referred shortcomings. Some of the terpolymer solutions were not stable at temperatures immediately above the cloud point, but aggregation occurred at an extremely low rate. Therefore, it was not feasible to perform the experiments at a scanning rate lower enough to not influence the turbidimetry curves because it would require very long measurement times. The curves slope can still be used to compare the aggregation rate, providing that the measurements were done at the same scanning rate. In this sense, we did all temperature scanning measurements at a constant rate of 1 °C/min.

In general, water solutions of the terpolymers remained clear at any temperature. The thermoresponsive behavior was only manifested in the presence of salts. Figure 1 shows the typical

(25) Gibbons, O.; Carroll, W. M.; Aldabbagh, F.; Yamada, B. *J. Polym. Sci., Polym. Chem.* **2006**, *44*, 6410.

(26) Zhang, C.; Easteal, A. J. *J. Appl. Polym. Sci.* **2003**, *88*, 2563.
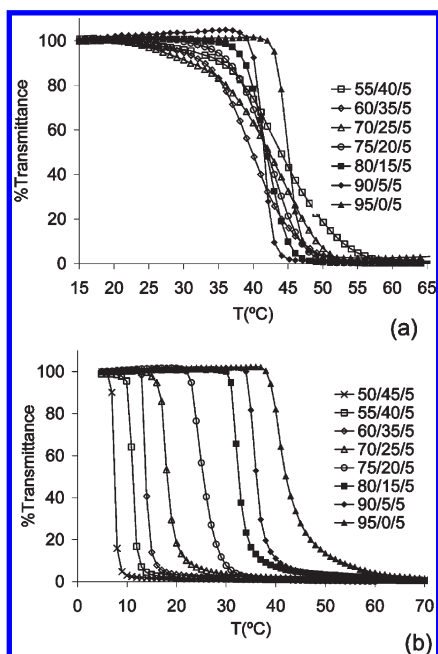
Figure 1. Turbidity curves showing the effect of copolymer composition on the macroscopic phase separation for heating (a) and cooling (b) scans (1 g/L, 0.154 M NaCl, 1 °C/min).
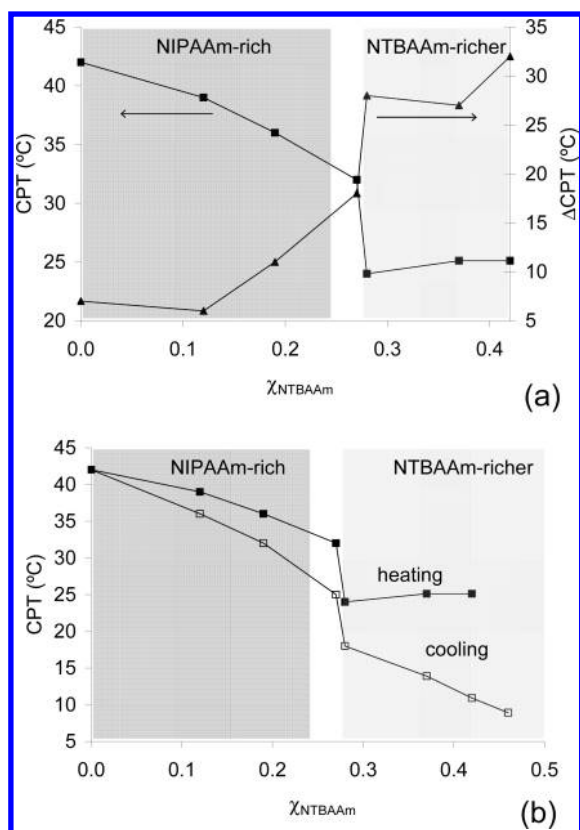
Figure 2. Cloud-point temperature (CPT) (filled squares) and macroscopic phase-separation sharpness (ΔCPT) (filled triangles) as a function of NTBAAm molar fraction (x_{NTBAAm}) (a). Comparison between CPT (filled squares) and redissolution temperature (empty squares) as a function of NTBAAm molar ratio (b).

temperature dependence of transmittance for solutions of copolymers with a rational composition variation, on both heating (Figure 1a) and cooling (Figure 1b). Figure 2a shows the cloud-point temperature extracted from Figure 1a and defined as the
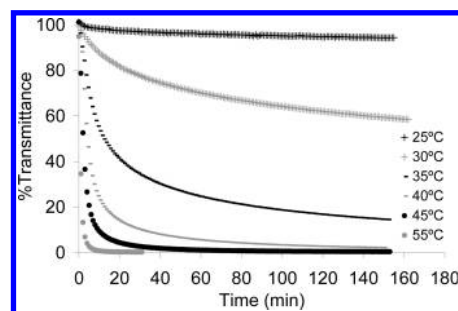
Figure 3. Isothermal aggregation kinetics of 60/35/5 (1 g/L) dissolved in 0.154 M NaCl aqueous solution at temperatures above the cloud-point temperature.

temperature at 98% light transmittance on heating. The phase separation sharpness was evaluated considering the temperature interval at which light transmittance changes from 98% down to 2% (ΔCPT) during the heating scan, and it is represented in Figure 2a as a function of the NTBAAm content.

It has been reported that linear NIPAAm homopolymer present a LCST around 31−33 °C in water[3−7] and that LCST is slightly depressed when NaCl is added at the concentration range used in this work.[10] When NIPAAm was copolymerized with a small amount of AMPS (95/0/5), i.e., a more hydrophilic (ionic) monomer, the CPT (∼42 °C) was raised as expected. The macroscopic phase separation is sharp and occurs in a narrow temperature range (Figures 1a and 2a). On the other hand, the CPT was reduced as expected by increasing the NTBAAm content, which results from an increased overall hydrophobic character of the copolymers (Figures 1a and 2a). Furthermore, it could be observed that as greater is the NTBAAm content on the copolymers, as slower is the aggregation process, leading to a decreased slope in the turbidity curves (Figure 1a) and consequently an increased ΔCPT (Figure 2a). It is interesting to notice that there is a composition interval (around 0.25−0.30 molar fraction of NTBAAm) at which the macroscopic phase separation changes from sharp to wide. Such alteration in the aggregation behavior is accompanied by an equally steep variation in the CPT. We have denominated these two composition ranges with very distinct aggregation behaviors as NTBAAm-richer and NIPAAm-rich polymers (shadowed areas of Figure 2). Considering that all copolymers possess identical charge (similar content of AMPS), the repulsive electrostatic forces are expected to be equivalent at the same ionic strength. Therefore, it is reasonable to conclude that the lower aggregation rate is only correlated with a higher NTBAAm (lower NIPAAm) content. This result is apparently contradictory with the colloidal aggregation principles. At the first glance, one could expect that the resultant of repulsive electrostatic and attractive hydrophobic forces would favor a faster aggregation process for the more hydrophobic NTBAAm-richer polymers.

Aggregation isotherms were determined for 60/35/5 (sample with broad aggregation profile), keeping the same polymer and NaCl concentrations (Figure 3). The temperature of the sample was rapidly increased to certain temperatures near and above the CPT, and transmittance values were measured with time. These measurements allowed us to elucidate that the studied system was not thermodynamically stable (or metastable) above the CPT and that broadening of turbidity variation was caused by temperature-dependent aggregation kinetics. Figure 3 shows that the turbidity increases continually with the time at all studied temperatures, but the process is much faster at higher temperatures, whereas aggregation is "virtually prevented" for temperatures

close to the CPT. According to these results, we could hypothesize that the observed decrease of the slope with increasing NTBAAm content does not mean that the volume transition became continuous. In fact, as we will discuss afterward, there is an observable discontinuous phase-separation process at the microscopic level.

Immediately after the heating scan, the copolymer solutions were subjected to a cooling step in order to study the redissolution temperature. The onset of the turbidity decrease in the redissolution curves might not be well-defined because settling of aggregates also contributes to decrease the turbidity. Hence, redissolution temperature was considered to be at 50% light transmittance to avoid the effect of settling. Besides, this option is further justified by the fast redissolution process observed for all the samples presented in Figure 1b.

As expected, the redissolution temperature decreases with increasing NTBAAm content in the terpolymer composition (Figure 1b), and it is always lower that the CPT (Figure 2b). The measured hysteresis is enhanced for NTBAAm-richer polymers. Moreover, as can be seen in Figure 1b, the curves of transmittance vs temperature in the cooling cycle are sharp for any ratio of NTBAAm, indicating that the redissolution occurs immediately below a certain temperature. The difference in the macroscopic phase-separation sharpness between heating and cooling scans can be understood in terms of electrostatic repulsion and hydrophobic attraction. During polymer aggregation the molecules charge density counteracts the hydrophobic forces, eventually delaying or hindering aggregation. When the system is cooled below the LCST, the copolymer rehydration cancels the attractive hydrophobic forces responsible for aggregates cohesion, and the electrostatic repulsion provides the driving force for the fast redissolution.

When plotting the redissolution temperature against the molar ratio of NTBAAm (Figure 2b), it was possible to observe an abrupt variation at the same composition range (0.25−0.30) in which a similar steep variation is observed for CPT and aggregation rate (Figure 2a). These observations motivated us to study the effect of the ionic strength and polymer concentration on the macroscopic phase separation for two different copolymers: one representative of the NTBAAm-richer polymer behavior (60/35/5) and the other typifying the NIPAAm-rich polymers (80/15/5).

Salt concentration might act both on the LCST and on the aggregation profile. Since both copolymers are polyelectrolytes, it was not surprising to observe that the ionic strength influences both polymers CPT in the same manner; when the NaCl concentration is increased, the CPT decreases (Figure 4). It was reported that, at the concentration range used in this study, the influence of NaCl in the pNIPAAm LCST is rather small (< 1 °C)[10,20] if compared with the reduction extent that we observed in the CPT for both terpolymers (> 30 °C). This divergence might indicate that the CPT is detected above the θ-temperature. If this is correct, the unexpectedly stronger dependence of the CPT on the NaCl concentration is related to the effect of salt concentration over the colloidal aggregation kinetics, rather than the θ-temperature. The addition of salt to the solution shields the repulsive Coulombic interactions between charged sulfonic groups (screening effect), facilitating colloidal aggregation if the system is above the θ-temperature. Although the CPT is similarly affected for both NTBAAm-richer and NIPAAm-rich copolymers, the transition rate is not equally affected. The turbidity rising rate strongly depends on the ionic strength for the more hydrophobic copolymer (60/35/5), being slower at lower salt content and more abrupt at higher concentrations. On the contrary, the ΔCPT is not affected by changes in the salt
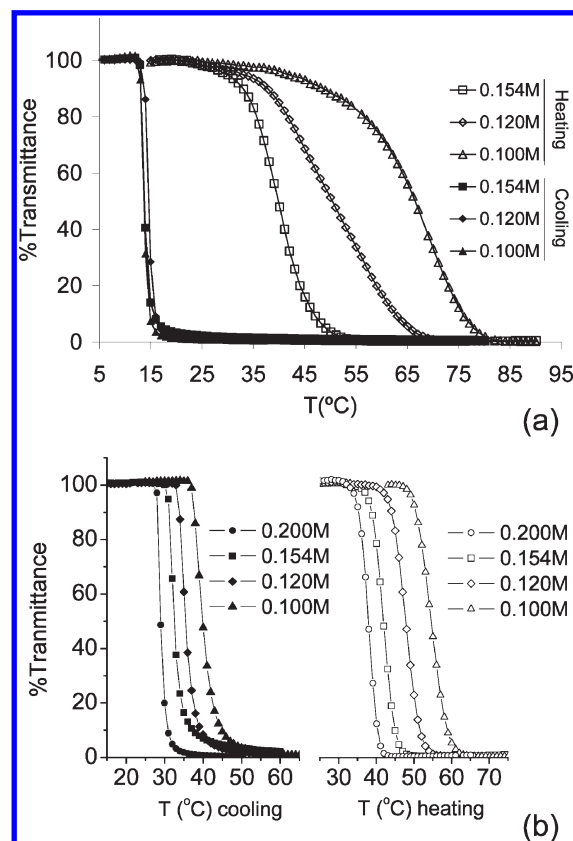
Figure 4. Effect of the NaCl concentration on the turbidity vs temperature curves on heating and cooling scans for 60/35/5 (a) and 80/15/5 (b). In both curves the polymers concentrations and scan rates were 1 g/L and 1 °C/min, respectively.

concentration for 80/15/5; in all cases a fast aggregation was observed. The strong dependence of the aggregation rate on the salt concentration for NTBAAm-richer polymers reveals that the colloidal stabilization effect is electrostatic in nature. Thus, why is this effect not observed for NIPAAm-rich polymers? A possible explanation is that, for NTBAAm-richer polymers, the stronger hydrophobic forces in action above the LCST are able to override the electrostatic potential energy increment caused by a higher charge density of the colloidal particles. In this situation, the increased charge density would provide an additional energy barrier for further colloidal aggregation, especially if charged segments were oriented toward the surface.

The effect of the ionic strength on the redissolution temperature was also evaluated (Figure 4). The NTBAAm-richer copolymer showed a fast redissolution profile for all tested salt concentrations. Moreover, the transmittance vs temperature curves are almost superimposed showing coincident redissolution temperature around 15 °C regardless of the ionic strength. On the other hand, a sharp redissolution profile was also observed for NIPAAm-rich polymers, but in this case the temperature at which the aggregates are redissolved depends on the salt concentration. Although a certain hysteresis was observed between heating and cooling, both aggregation and redissolution processes of the NIPAAm-rich polymer are influenced in a very similar extent by the solution ionic strength.

The dependence of the CPT on the polymer concentration is shown in Figure 5. In this case, the aggregation and redissolution behavior is very similar for NTBAAm-richer and NIPAAm-rich polymers. The aggregation rate increased and CPT decreased at higher polymer concentration, whereas the redissolution profile
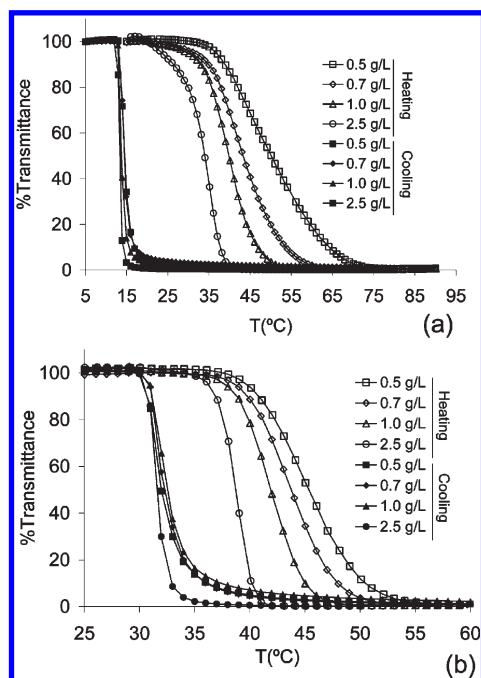
Figure 5. Effect of the polymer concentration on the transmittance vs temperature curves on heating and cooling scans for 60/35/5 (a) and 80/15/5 (b). In both curves the salt concentrations and scan rates were 0.154 M and 1 °C/min, respectively.
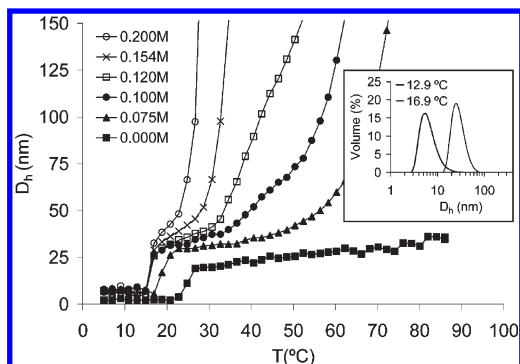
Figure 6. Temperature dependence of the apparent hydrodynamic diameter (D_h) at several NaCl concentrations for 60/35/5 (polymer concentration 1 g/L). The inset shows the hydrodynamic diameter distribution at temperatures before and after the aggregation (0.120 M NaCl).

was fast and not dependent on the polymer concentration. The results are in agreement with the general principles of colloidal aggregation, where the aggregation is dependent on the particle concentration. In turn, disaggregation should be mainly ruled by particle intrinsic structural features.

Since some of the studied polymer solutions do not present sharply defined cloud points, we used dynamic light scattering (DLS) in order to elucidate the apparently contradictory behavior observed with the copolymer composition (more hydrophobic polymers showed lower aggregation rates). DLS permits the analysis of size variations at the molecular scale, and therefore, it is possible to analyze early stages of aggregation. Figure 6 shows the temperature dependence of apparent hydrodynamic diameter (D_h) on the NaCl concentration for 60/35/5, at a fixed polymer concentration of 1 g/L. It could be observed that in the absence of salt a sharp increase of D_h is observed at 23 °C, indicating the aggregation of individual ionomer chains in solution. Above this temperature value, the D_h increases slightly with the temperature.

The formed colloidal particles remained stable at 27 °C for at least 11 h (result not shown). Qiu et al. reported a similar behavior for low molecular mass poly(*N*-isopropylacrylamide-*co*-acrylate) in water at a comparable concentration.[27] They suggested that when short chains are analyzed by DLS, the intrachain collapse is not observed since its effect on the overall chain dimension is negligible and is faster than the interchain aggregation. Because of this reason, the decrease on D_h due to the coil-to-globule transition typically observed for larger polymers in very diluted solution[4,6,7] was not observed for the studied terpolymers with shorter chains. Even though the coil-to-globule transition is not observed, this first aggregation step should be very close to the θ-temperature,[9] providing our best estimation of the LCST. Being so, we will use the term LCST to denominate this early aggregation observed by DLS and the CPT to denote only the value obtained by turbidimetry, for the sake of clarity.

When NaCl was added to the solution, a similar early aggregation behavior was observed, but the aggregates were not stable in the entire temperature range, ultimately leading to a further increase of the D_h above a certain temperature. Comparing the CPT (Figure 4a) with the LCST (Figure 6) of 60/35/5 at several NaCl concentrations, it is possible to see that there is no correspondence between both values. This observation raises great concerns on the use of turbidimetry to evaluate the LCST of charged polymers. In fact, CPT is related with the massive aggregation observed in Figure 6 at higher temperatures, being the first formed metastable aggregates (LCST) undetected by turbidimetry. If in our results the CPT does not match precisely the temperature at which a more pronounced D_h increment is observed, it is because scanning rate is lower in the DLS measurements due to the relatively longer times required for data acquisition and temperature stabilization. The gap between the metastable nanosized aggregates (LCST) and the faster aggregation (CPT) is more pronounced at lower salt concentrations. When salt concentration increases, the stability range of the colloidal particles decreases. Thus, it is reasonable to conclude that the effect of NaCl concentration on the CPT is solely related with the screening effect over the charge, reducing colloidal stability and accelerating aggregation. Hypothetically, the LCST dependence on the NaCl concentration can only determine the temperature at which the first metastable aggregates are formed.

The inset in Figure 6 shows the hydrodynamic diameter distribution at temperatures immediately before and after the aggregation when 0.120 M NaCl was added to the solution. At 12.9 °C, slightly below the LCST, only one peak centered at ∼8 nm was observed. This peak corresponds to individual copolymer chains, as it was confirmed by measuring the size distribution of the polymer in a good solvent (tetrahydrofuran). The obtained volume−D_h distribution was equivalent to that obtained in water below the LCST (graph not shown). The size distribution above the LCST at 16.9 °C is narrower and corresponds to an average D_h of ∼25 nm, reflecting the interchain aggregation.

The stability of the aggregates before the massive aggregation was tested isothermally by measuring the D_h and the scattered light intensity with the time at set temperatures close to the LCST (Figure 7). The light intensity is very sensitive to small changes in the scatters size and should be constant, at fixed scattering angle and temperature, if there is no aggregation. 60/35/5 in 0.120 M NaCl showed the first aggregation at ∼15 °C (Figure 6), and it could be observed that at 19 °C both D_h and light intensity are stable for at least 11 h (Figure 7). However, when the solution was

(27) Qiu, X. P.; Kwan, C. M. S.; Wu, C. *Macromolecules* **1997**, *30*, 6090.
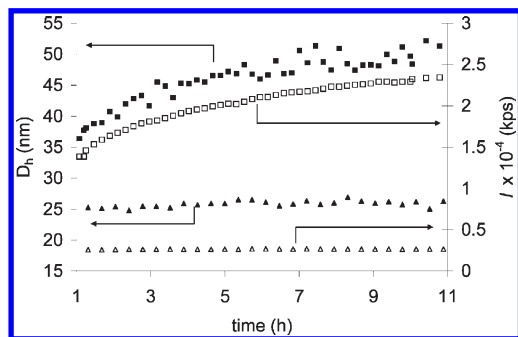
Figure 7. Isothermal aggregation kinetics of 60/35/5 determined by DLS (1 g/L polymer concentration and 0.120 M NaCl) at 19 °C (triangles) and 25 °C (square). Filled symbols represent the hydrodynamic diameter, and empty symbols represent scattered light intensity (173°).
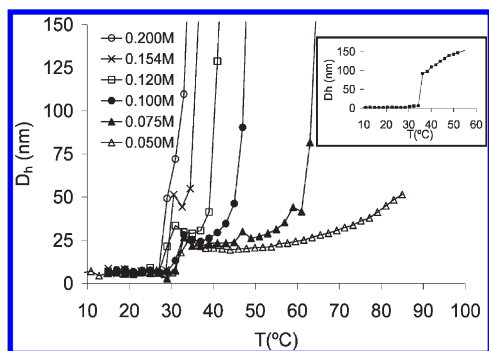
Figure 8. Temperature dependence of the apparent hydrodynamic diameter (D_h) at several NaCl concentrations for 80/15/5 (polymer concentration 1 g/L). The inset shows the temperature dependence of D_h in water.

left at 25 °C, the light intensity and D_h increased with the time, indicating that aggregation occurs at this temperature. It seems that the aggregation rate increases continuously with the temperature, so that a limit between two aggregation regimes is not well-defined. In this sense, the separation of the aggregation behavior in two stages, early metastable aggregation and later massive coagulation, is merely descriptive.

It is interesting to notice that the temperature observed for the first aggregation in DLS (LCST) corresponds to the redissolution temperature observed by turbidimetry. Hence, for this specific case, we can state that the redissolution temperature is more representative of the LCST than the CPT. On the other hand, after the massive coagulation the produced aggregates are stable in the cooling scan; i.e., there is no redissolution as long as the temperature is kept above the LCST.

The LCST of the NIPAAm-rich polymer (80/15/5) (Figure 8) was higher than the LCST of 60/35/5 for all tested NaCl concentration, as expected. A quite different behavior was observed for 80/15/5 water solution (inset graph). Substantially bigger scatters are detected at the first aggregation, which increases continuously with the temperature, but never reaching a massive coagulation stage.

The lower percentage of NTBAAm monomer in this copolymer composition should imply that weaker hydrophobic aggregation forces are active above the LCST. Therefore, hydrophobic interactions may not be able to bring the charges close enough to provide an effective surface charge density, hindering electrostatic stabilization of the aggregates. Interestingly, when small quantities of salt are added to the solutions, it could be observed that the formed aggregates were smaller and showed an early

metastable aggregation stage, recalling the aggregation behavior observed for NTBAAm-richer polymer. This supports the explanation given before, since the screening effect produced by the added salt are expected to reduce electrostatic repulsion inside the aggregates. In this sense, there should be a salt concentration in which the cohesive hydrophobic forces are sufficient to overcome the reduced internal repulsion and provide an effective surface charge density for colloidal stabilization.

Comparing Figure 6 and Figure 8, we can conclude that both polymers showed similar behavior with the formation of small aggregates that remain stable at lower temperature, after which a massive coagulation occurs. However, the coagulation rate showed a sharper acceleration for NIPAAm-rich than for NTBAAm-richer samples. Another common feature of both samples is that the CPT determined by turbidimetry is not representative of the LCST for any tested condition; nanosized aggregates are always observed by DLS at lower temperatures than the CPT determined by turbidimetry. In some cases, as for low salt concentrations, the observed differences could be as great as 30 °C. Nevertheless, the comparison of DLS and turbidity results for NIPAAm-rich polymer showed that the redissolution of the bigger aggregates occurs at temperatures higher than the LCST. On the other hand, when the same comparison is performed for NTBAAm-richer polymer, we could observe that the aggregates formed at higher temperatures only disaggregate in the cooling ramp when the LCST is reached. This observation confirms that the internal cohesion of 60/35/5 formed aggregates is enough to compensate the electrostatic repulsion at any temperature above the LCST. In NIPAAm-rich polymer the hydrophobic interactions are weaker and the aggregates are redissolved at temperatures higher than the LCST. Moreover, it is interesting to notice that for this polymer (80/15/5) the redissolution temperature changed with the salt concentration. Increasing salt concentration results in the enhancement of charge screening, and subsequently the electrostatic repulsion is progressively reduced. Therefore, the hydrophobic interactions are enough to support the aggregates stability at lower temperatures.

Conclusions

p(NIPAAm-*co*-NTBAAm-*co*-AMPS) aqueous solution did not show turbidity changes (macroscopic phase separation) with the temperature. The CPT was only observed when NaCl was added to the solutions. However, the formation of metastables nanosized aggregates (LCST) was observed by DLS in both water and aqueous saline solutions. The macroscopic phase separation is always observed at higher temperatures than the formation of the nanoaggregates. Therefore, there is no correlation between CPT and LCST. These results raise serious concerns about the validity of using turbidimetry measurements to obtain a reliable estimation of the LCST for charged thermoresponsive polymers.

Both the CPT and the LCST decreased with the increase of hydrophobicity (increased NTBAAm content). However, the aggregation profile observed by turbidimetry dramatically change above a critical amount of NTBAAm (0.25−0.30). Terpolymers with NTBAAm content below the critical value showed a fast macroscopic phase separation for all studied conditions. Moreover, the formed large aggregates redissolve in the cooling ramp at different temperature depending on the salt concentration and always at temperatures higher than the LCST. On the other hand, NTBAAm-richer terpolymers showed a slower aggregation process whose rate was found to depend on salt concentration. In this case, the formed large aggregates during the heating scan disentangled always at the same temperature which is coincident with

the LCST. The differences observed on copolymers solutions can be explained as the result of a fine balance between hydrophobic attractive forces and electrostatic repulsion, which leads to formation of intermediate metastable nanosized aggregates. The hydrophobic cohesion forces for polymers with higher NTBAAm content are stronger, thus able to withstand a higher surface charge density. Therefore, the aggregation is slower due to the electrostatic repulsion that acts as stabilizer of the aggregates. Furthermore, the redissolution only occurs at the LCST because the stronger internal cohesion is enough to compensate the electrostatic repulsion. On the other hand, the hydrophobic forces in polymers with lower content of NTBAAm are weaker and not able to bring charges close enough to provide an effective surface charge density, hindering electrostatic stabilization of the aggregates with a consequent fast coagulation. Moreover, the larger aggregates formed meanwhile are redissolved before reaching the LCST in the cooling ramp because the hydrophobic interactions are not strong enough to counteract the electrostatic repulsion.